Accepted Manuscript

Monte Carlo simulations of enzymatic reactions in crowded media. Effect of the enzyme-obstacle relative size

Laura Pitulice, Eudald Vilaseca, Isabel Pastor, Sergio Madurga, Josep Lluís Garcés, Adriana Isvoran, Francesc Mas
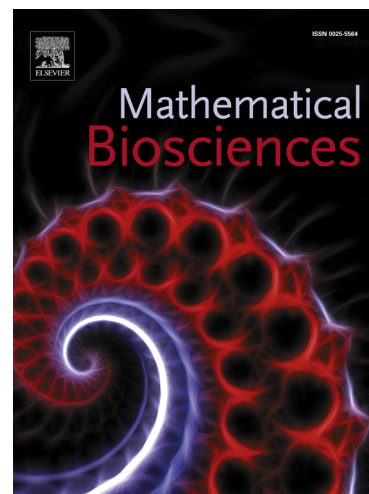
Please cite this article as: L. Pitulice, E. Vilaseca, I. Pastor, S. Madurga, J.L. Garcés, A. Isvoran, F. Mas, Monte Carlo simulations of enzymatic reactions in crowded media. Effect of the enzyme-obstacle relative size, *Mathematical Biosciences* (2014), doi: http://dx.doi.org/10.1016/j.mbs.2014.03.012

Monte Carlo simulations of enzymatic reactions in crowded media.

Effect of the enzyme-obstacle relative size

Laura PITULICE[a,b], Eudald VILASECA[c], Isabel PASTOR[c], Sergio MADURGA[c], Josep Lluís GARCÉS[d], Adriana ISVORAN[a] and Francesc MAS[c,*]

[a]*Department of Biology-Chemistry, West University of Timisoara, Pestalozzi 16, 300311, Timisoara (ROMANIA) (Permanent address)*

[b]*University Al.I. Cuza from Iaşi, 11 Carol I, Iasi (ROMANIA) (temporary affiliation)*

[c]*Physical Chemistry Department and Research Institute of Theoretical and Computational Chemistry (IQTCUB) of Barcelona University (UB), C/ Marti i Franquès, 1, E-08028, Barcelona (Catalonia, SPAIN)*

[d]*Chemistry Department, University of Lleida (UdL), Lleida (Catalonia, SPAIN)*

[*] Corresponding author:

Francesc Mas

Address: C / Martí i Franquès, 1, 08028 BARCELONA (SPAIN)

E-mail: fmas@ub.edu

Fax: (+34) 934021231

Running title: Enzymatic reactions in crowded media

Abstract

We perform Monte Carlo simulations in three-dimensional (3D) lattice in order to study diffusion-controlled and mixed activation-diffusion reactions following an irreversible Michaelis-Menten scheme in crowded media. The simulation data reveal the rate coefficient dependence on time for diffusion-controlled bimolecular reactions developing in three-dimensional media with obstacles, as predicted by fractal kinetics approach. For the cases of mixed activation-diffusion reactions, the fractality of the reaction decreases as the activation control increases. We propose a modified form of the Zipf-Mandelbrot equation to describe the time dependence of the rate coefficient, $k(t) = k_0 (1 + t/\tau)^{-h}$. This equation provides a good description of the fractal regime and it may be split into two terms: one that corresponds to the initial rate constant (k_0) and the other one correlated with the kinetics fractality. Additionally, the proposed equation contains and links two limit expressions corresponding to short and large periods of time: $k_1 = k_0$ (for $t << \tau$) that relates to classical kinetics and the well-known Kopelman's equation $k \sim t^{-h}$ (for $t >> \tau$) associated to fractal kinetics. The τ parameter has the meaning of a crossover time between these two limiting behaviours. The value of k_0 is mainly dependent on the excluded volume and the enzyme-obstacle relative size. This dependence can be explained in terms of the radius of an average confined volume that every enzyme molecule feels, and correlates very well with the crossover length obtained in previous studies of enzyme diffusion in crowding media.

2

1. Introduction

Many functions of living cells involve complex biochemical reactions of which rates must be as fast as possible to allow a wide range of processes to take place. To study biochemical reactions one must take into account that cellular media are not homogenous but highly compartmented being characterized by a high total macromolecular content known as macromolecular crowding [1-3]. Macromolecular crowding influences the thermodynamics of the cell by volume exclusion effects [1-3]. It also affects the diffusion processes by reducing the diffusion coefficient of the macromolecules [4-20]. In this way, diffusive processes leading to the necessary encounter of reactants determine the rates of biochemical reactions. However, after the pioneering work of Laurent in 1971 [21], quite a few studies have explored the effects of crowding on enzyme catalysis, even *in vitro* [22-39].

Schnell and Turner [40] excellently reviewed a few non-classical approaches regarding biochemical reactions developing in crowded media. They are mainly divided into deterministic approaches, particularly comprising fractal kinetic approaches [41-42] and kinetics based on fractional reaction orders [43-46], and stochastic ones [47]. However, there are mathematical connections between deterministic and stochastic models. The conversion between these models has been illustrated for large-scale genetic regulatory networks [48] and for Michaelis-Menten enzyme kinetics and stochastic focusing [49]. The deterministic models proved to be widely applied on the analysis of enzymatic reactions developing in crowded media. Among them, the fractal-like kinetics is the one considered in the present study. The fractal-like kinetics assumes that the rate coefficient describing diffusion controlled chemical reactions is time dependent, for large periods of time, taking the form [41-42]:

$$k(t) = k_0^{\cdot} t^{-h} \quad ; \quad 0 \leq h \leq 1 \tag{1}$$

This formalism brakes down for $t \to 0$ and $h > 0$ because in this situation $k(t) \to \infty$. A solution has been proposed by Schnell and Turner [40] and they consider a modified fractal-like kinetics with the rate coefficient following a temporal Zipf-Mandelbrot distribution:

$$k(t) = \frac{k_0^{''}}{(\tau + t)^h} \quad ; \quad 0 \le h \le 1 \tag{2}$$

In both Eqs. 1 and 2, $k_0^{'}$ and $k_0^{''}$ are constant even though not related to any rate constant as in classical kinetics and h, called the fractal parameter, depends on the topological dimensionality of the medium in which reaction occurs. The τ parameter in Eq. 2 is a positive constant and its physical meaning is the time after which the reaction "feels" the crowding effects [40].

Recently, Bajzer at al. [44-46] have proven that Schnell and Turner model applied on bimolecular reactions predicted an unlikely asymptotic concentration of the product. This approach is valid for diffusion-limited reactions and we used it in our investigation assuming that the corresponding time period of our simulations does not reach the asymptotic region. Moreover, for enzymatic reactions in crowded media, the diffusion-limited case is not the most usual one [16, 33, 38 and references quoted therein]. There are also cases of mixed activation-diffusion control, e.g. the reduction of Pyruvate by NADH catalyzed by Lactate Dehydrogenase induced by Dextrans [39]. For these last cases, the asymptotic concentration of the product is reached at longer periods of time than for diffusion-limited reaction cases and, thus, the time period used in simulations can be larger.

To perform *in vivo* experiments of biochemical reaction dynamics in crowded media is a difficult task, therefore computer simulation is an excellent alternative. There are numerous published papers with regard to simulations of diffusion processes [4-7, 10-12, 17, 19-20] and chemical reactions in crowded media [40-47, 50-56]. Macromolecular crowding

can lead to anomalous diffusion more likely when low dimension environments are considered especially up to percolation threshold [41]. In such cases, diffusion is strongly influenced by crowders concentration, size and mobility. It has been illustrated that diffusion becomes more anomalous when higher concentration of obstacles is present but less anomalous for mobile and big obstacles [10-12, 14, 17-20]. Inside living cells, macromolecular crowding does not always reach the percolation limit. However, when large macromolecules diffuse inside the cell their movement is greatly impaired [8, 15]. Consequently, anomalous diffusion becomes perceptible and significant giving rise to rate-limited chemical reactions [16].

Berry [52] studied a native Michaelis-Menten reaction scheme using a Monte Carlo simulation on two-dimensional lattice with cyclic boundary conditions. He used immobile obstacles varying their densities from zero to the percolation threshold. His study showed that the reaction kinetics was of fractal type as a result of low-dimensional media and macromolecular crowding. The kinetics fractal characteristics intensified with obstacles density and substrate concentration, the two contributions being mainly additive.

Schnell and Turner [40] used Berry's algorithm and implemented it in a two-dimensional lattice with cyclic boundary conditions using the same parameters [52]. Apart from confirming the clear decay of the rate coefficient k_1 over time, they also revealed that the rate coefficient behaviour at $t \rightarrow 0$ was better described by the Zipf-Mandelbrot distribution than the Kopelman's law. They extended the simulation to a three-dimensional lattice without obstacles for which case the rate coefficient did not show an apparent dependence on time, being thus in accordance with classical kinetics.

Isvoran and co-workers [57] analysed several computational aspects of the implementation of Berry's algorithm in two-dimensional media with obstacles. Particularly, different initial distributions of obstacles and reactants molecules were considered and also

6

the effect brought by eight nearest neighbours of every particle in the lattice instead of four. Moreover, Isvoran and co-workers [58] compared different equations proposed in the literature in order to describe the rate coefficient time dependence.

Agrawal and co-workers [59] studied the effect of macromolecular crowding on Michaelis-Menten enzymatic reaction occurring in 2D media. They used a Monte Carlo algorithm based on substrate molecules random walk in a percolation cluster. The substrate diffusion length and the reaction rate decrease as the fractional volume occupancy of the crowding agent increases.

Intracellular structures have been explicitly modelled using immobile/mobile obstacles in 2D environments for the first time by Grima and Schnell [55]. They compared different geometries of the simulation grid with an off-lattice Brownian Dynamics, revealing qualitative and quantitative differences as the obstacle concentration increased. Moreover, Grima [56] extended the off-lattice simulation study to the case of activation control in crowded media, showing that crowding induces a reduction of the noise of intracellular biochemical reactions. Recently, Klann and coworkers [60] have developed an off-lattice continuous space simulation method, in which all sub-cellular structures are modelled explicitly as static obstacles. They noticed a reduced reaction rate in presence of obstacles. They also identified some factors causing the diminution of the reaction rate: the reduced mobility of the reactants and molecular crowding determining a reduced accessibility of the molecules.

Moreover, there are some computational and theoretical papers emphasising the effect of diffusion on enzyme kinetics in cellular environment [61-65 and references therein]. These studies provide several expressions concerning the time-dependence of reactants diffusion coefficients and the effects of the excluded volume resulting in time-dependent rate coefficients.

7

In recent years, the effects of crowding on enzyme catalysis have been explored by different experimental works, excellently depicted by Zhou et al [16] and Noris and Malys [30]. Some of the studies present distinct effects produced by various crowding agents on the enzymes kinetics [26, 33, 38-39, 66]. These effects are given by different experimental conditions considering the type, shape, size and excluded volume of the used crowders. Anyway, most of the investigations indicate that the effect of excluded volume due to the presence of crowding agent is the major player in modulating enzymatic behavior.

However, the dependence of the kinetic parameters of a typical Michaelis-Menten enzymatic mechanism on the enzyme-crowder relative size and their particular shape is not yet well understood.

As a result, the present study aims at extending Berry's algorithm in order to examine a more nature-like environment, namely to analyse an irreversible Michaelis-Menten enzymatic reaction progressing in 3D crowded media, not only for diffusion-limited reaction cases but also for mixed activation-diffusion control ones. In detail, the work attempts to express the time-dependence of the bimolecular rate coefficients in terms of excluded volume and enzyme-obstacle relative size. A modified form of Zipf-Mandelbrot equation, previously proposed by our research team [67], is used to describe the time dependence of the rate coefficient $k(t) = k_0 \left(1 + t/\tau \right)^{-h}$. Recently, this kind of equation has also been taken into account by Bajzer and co-workers [46]. They also generalize different approximations used in the literature in order to understand which kind of formalism better describes the biochemical reactions in crowded environment, and used them in an experimental study to test different models for reaction kinetics in intracellular environments [46].

2. Theoretical background

We apply the fractal kinetics approach on the irreversible Michaelis-Menten mechanism of enzymatic reactions. It considers the following reactions

$$E + S \underset{k_{-1}}{\overset{k_1}{\Leftrightarrow}} C \overset{k_2}{\rightarrow} E + P \tag{3}$$
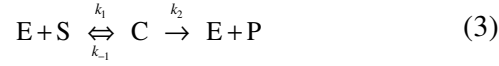
where E is the enzyme, S the substrate, C the enzyme-substrate complex, P the product and k_i are the rate constants.

The fractal kinetics considers that second order reactions are described by time dependent rate coefficients. In the Michaelis-Menten mechanism only the first reaction $E + S \overset{k_1}{\Rightarrow} C$ is a reaction of a second order, so only k_1 depends on time in crowded media [41].

The Zip-Mandelbrot Eq. 2 proposed by Schnell and Turner [40] has been shown to describe well enough the temporal dependence of k_1. However, for $t \rightarrow 0$ the equation becomes $k(t) \rightarrow k_0^{"} \tau^{-h}$ where $k_0^{"}$ does not correspond to the rate constant described by classical kinetics, neither by dimensionality nor by being independent of the reaction environment. Therefore, we proposed a modification of Eq. 2 [67] and write it as

$$k(t) = k_o \left(1 + \frac{t}{\tau}\right)^{-h} \tag{4}$$

where $\tau > 0$ and $h > 0$. Now, for $t \rightarrow 0$ we obtain

$$\lim_{t \rightarrow 0} k(t) = k_0 \tag{5}$$

which corresponds to the initial rate constant of the bimolecular reaction which is time independent as in classical kinetics. In addition, for $t \gg \tau$ we may neglect the number 1 in Eq. 4 and it becomes

$$\lim_{t \gg \tau} k(t) = k_0 \tau^h t^{-h} = k_0^{'} t^{-h} \Rightarrow k_0^{'} = k_0 \tau^h \tag{6}$$

9

being similar with Kopelman's equation [41-42] and having the same problem of dimensionality of the $k_0^{'}$ parameter, which does not correspond to the rate constant in classical kinetics.

However, a mathematical description in terms of macromolecular crowding of the two limiting situations of Eq. 4 is necessary. On the one hand, we need to generalize the well-known solution of Smoluchowski equation for the rate constant of bimolecular reactions in 3D homogeneous media in infinite dilute conditions [68]

$$k_d^\infty = 4\pi N_A D_{ES} r_{\min} \tag{7}$$

for diffusion-limited reactions taking place in crowded media. In this equation D_{ES} refers to the relative diffusion coefficient between the E and S reactant molecules ($D_{ES} = D_E + D_S$) and $r_{\min}$ is the distance of maximum approach between the reactant molecules, considered as spherical particles, for a reactive collision ($r_{\min} = r_E + r_S$). We suppose that macromolecular crowding is seen as a division of the system in small volumes surrounded by big obstacles. This is due to the fact that the free volume of the reaction media, $V(1-\phi)$, is lower than the total volume, V, because of the excluded volume, ϕ, caused by the crowding macromolecules. The shape and number of these divisions should depend on the density, size and way of distribution of the obstacles. For each division it is possible to consider an average volume, which is a decreasing function of the excluded volume, ϕ. Then, if we consider r_{cv} the radius of this average small volume (confined volume), the stationary profile of substrate S molecules towards one of enzyme E molecule (described by the Laplace equation in spherical coordinates; $\nabla^2 c_S(r) = \dfrac{d^2 c_s}{dr^2} + \dfrac{2}{r}\dfrac{dc_s}{dr} = 0$) is limited by the distance of maximum approach ($r_{\min}$), where the substrate concentration vanishes, and the radius of the confined volume (r_{cv}), where the substrate concentration has the average effective value within the

10

confined volume, c_S^{eff}. In these conditions, it is straightforward to integrate the Laplace equation for substrate concentration, to obtain the stationary profile of the substrate [68]:

$$c_S(r) = c_S^{eff}\left(\frac{r_{cv}}{r_{cv} - r_{min}}\right)\left(1 - \frac{r_{min}}{r}\right) \tag{8}$$

Now, the total diffusion flux of substrate S molecules at maximum approach distance, r_{min}, for every enzyme E molecule, is

$$J_{dif,total}(r_{min}) = -4\pi\, r_{min}^2 N_A D_{ES}\left(\frac{\partial c_S}{\partial r}\right)_{r=r_{min}} = 4\pi\, r_{min} N_A D_{ES} c_S^{eff}\left(\frac{r_{cv}}{r_{cv} - r_{min}}\right) \tag{9}$$

Then, the rate of the bimolecular reaction that takes place in any confined volume, can be put in terms of the total diffusion flux of substrate S molecules

$$J_{reaction} = k_d c_E^{eff} c_S^{eff} = J_{dif,total}(r_{min}) c_E^{eff} \tag{10}$$

where c_E^{eff} is the average effective concentration of the enzyme E molecules within the confined volume.

Thus, combining Eqs. (9) and (10), it is straightforward to obtain a relationship between the diffusion-limited rate constant, k_d, and the radius of the confined volume

$$k_d = 4\pi\, r_{min} N_A D_{ES}\left(\frac{r_{cv}}{r_{cv} - r_{min}}\right) = k_d^\infty\left(\frac{r_{cv}}{r_{cv} - r_{min}}\right) \tag{11}$$

We may notice from Eq. 11 that the diffusion-limited rate constant, k_d, increases as the radius of the confined volume, r_{cv}, decreases. As a result, the k_0 parameter in Eq. 4 can be interpreted as the diffusion-limited rate constant, k_d, which describes the reaction at initial times when it takes place within a confined volume, as being in an homogenous medium:

$$k_0 \equiv k_d = k_d^\infty\left(\frac{r_{cv}}{r_{cv} - r_{min}}\right) = k_d^\infty f(r_{cv}) \tag{12}$$

However, the dependence of the confined volume radius (r_{cv}) on crowding conditions is not easy to be expressed in this simplified mean-field approximation. Previous studies of

11

enzyme diffusion in crowding media [19] show that there are a crossover length, $r* \equiv \sqrt{\tau * D_E^*}$, that represents the minimum displacement distance from which the diffusion of enzymes becomes normal, before a period of time, $\tau *$, that is anomalous, and achieve a constant diffusion coefficient, D_E^*, lower than its value at infinite dilution, D_E. This crossover length depends on both the exclude volume and the size of the obstacle. However, it is not easy to obtain a simple mathematical function for it.

In order to work with dimensionless parameters, we use a dimensionless length for the sites of the simulation lattice, associated to the mean free path covered by one substrate molecule, λ, in a Monte Carlo time step, $\tilde{t}$. This two parameters can be related using the Einstein-Smoluchowski equation in 3D: $\lambda^2 = 6D_S\tilde{t}$. Therefore the time-dependent rate coefficient, $k(t)$, and the rate constants, k_0 and k_d, have dimensionless values dependent on the dimensionless rate constant of bimolecular reactions in 3D homogeneous media in infinite dilute conditions, Eq. 7:

$$\tilde{k}_d^\infty = \frac{2\pi r_{\min} D_{ES}}{3\lambda D_S} \tag{13}$$

The later depends on the size and diffusion coefficient of the substrate and enzyme molecules considered in infinite dilute conditions.

Then, from the dimensionless version of initial rate constant of the modified Zipf-Mandelbrot, defined in Eq. 4 and given by Eq. 12, the dependence on the confined volume, $f(r_{cv})$ defined in Eq. 12, is obtained as the ratio between the initial rate constant of the modified Zipf-Mandelbrot equation and the rate constant of bimolecular reaction of enzyme-substrate in 3D homogeneous media

$$\frac{k_0}{k_0^\infty} = \frac{\tilde{k}_0}{\tilde{k}_0^\infty} = f(r_{cv}) = \left(\frac{r_{cv}}{r_{cv} - r_{\min}}\right) \tag{14}$$

which depends on the excluded volume and enzyme-obstacle relative size.

In order to simplify the notation, in the following sections we will not use the "~" sign for the dimensionless parameters.

3. Methodology

3.1 Simulation algorithm

The Michaelis-Menten enzymatic reaction in 3D obstructed media was modelled as a reactive process among particles moving in a 200x200x200 three-dimensional lattice with cyclic boundary conditions. The obstacles (O) are randomly distributed and their density is under the percolation threshold. Several test simulations performed for different lattice sizes yielded the same results (data not shown here). The simulation algorithm is an extension of the algorithm developed by Berry [52].

According to Michaelis-Menten scheme (Eq. 3) in presence of crowding agents, there are five different types of molecules distributed in the lattice: substrate (S), enzyme (E), complex (C), product (P) and obstacle (O). The S, E, C and P molecules can move through the lattice performing a random walk. The obstacle particles (O) are non-reactive species and are kept fixed during the simulation.

We consider excluded volume interactions (hard-sphere repulsions) among diffusing particles, so any site in the lattice may not be occupied by two particles at the same time, excepting the S and P particles, which are allowed to share the same lattice site. During the simulation process there are lattice sites that are occupied by one or several S molecules and/or one or several P molecules. In fact we are considering S and P molecules being smaller than a lattice site. Every C and E particle is considered to occupy a single lattice site. In contrast, to account for the usual greater size of the crowding molecules and to analyse the effect of the relative crowder size in the diffusion-reaction process, four different obstacles sizes have been considered (see Fig. 1 of Ref. 19): 1 site, 27 sites (a 3x3x3 site cube), 81 sites (a cube of 5x5x5 sites with edge and vertex sites removed to obtain a quasi-spherical shape)

and 179 sites (a cube of 7x7x7 sites with edge and vertex sites removed). We use the notation 5x5x5 R and 7x7x7 R (where R stands for rounded) to refer to the last two obstacle sizes. As every obstacle occupies many sites within the lattice, in our calculations we distinguish the density of sites occupied by obstacles, [O]$_{sites}$ from the concentration of obstacle particles, [O]. We will refer to the density of sites occupied by obstacles, [O]$_{sites}$, as the excluded volume due to the obstacle presence (ϕ). Four values for the obstacle excluded volume have been considered: 0.1, 0.2, 0.3 and 0.4.

The rate constants k_1, k_{-1} and k_2 are modelled by the reaction probabilities f, r and g, respectively. We have considered f=1, r=0.02 and g=0.04 for diffusion-limited reaction case, similarly with previous simulations presented in the literature [40,52], and f=0.75, 0.50, 0.25 for mixed activation-diffusion control case. In order to estimate the values of these parameters with biophysical importance, we can assume that the mean free path of a typical enzyme, with R_g=(2-4) nm and D_E= 2×10^{-10} m^2 s^{-1} [69], is λ = 5 nm. Additionally, taking into account the relationship between dimensionless and dimensional rate constants explained in Sec. 2, it is possible to obtain the ratio between dimensionless and dimensional k_2/k_1 in terms of $N_A\lambda^3$. Then, for a typical enzymatic reaction [33], with $k_1 \approx k_2/K_M$ = (1-3) $\times 10^5$ M^{-1} s^{-1}, being $K_M \equiv (k_2 + k_{-1})/k_1$ the Michaelis constant, k_2 = 2×10^2 s^{-1}, and $k_{-1} \le k_2$, we obtain k_2/k_1 = (0.02-0.05), which are of the same order as the above considered probabilities. The value of k_1 lies in the region of diffusion-limited reaction of the proposed spectrum of protein-protein association rate constant [69-70]. Its value is also in agreement with the statistical study of Bar-Even et al. [71] regarding kinetic parameters of the majority of enzymes, which are below the diffusion-limited rate of a typical bimolecular reaction taking place between low-molecular mass reactants, in diluted solutions [68, 71].

The rules for the movement and reaction depend on the type of molecule. One molecule is chosen randomly to move or react according to the following rules:

- if the selected molecule is S, a destination site is chosen randomly within the 6 neighbouring positions; if this site is empty or occupied with S or P, the molecule moves to the new position; if it is occupied by C or O, the molecule rests in the old position; if it is occupied by E, a reaction occurs according to the f probability. In that case the destination molecule is replaced by C and the S molecule is removed.

- if the selected molecule is E, first the probability of its movement is checked. If the motion is accepted, a random direction is picked and all neighbouring sites are analysed. If one of these sites contains an S the reaction occurs according to the f probability. Thus, E is replaced by C preserving the same position, and S is removed. On the contrary, when the sites are empty the displacement of E is performed. The displacement will be impeded only by the presence of any other particle instead S.

- if the selected molecule is C, a site among its neighbour empty sites is randomly chosen. If this C has not empty neighbours, we choose randomly another C [57]. According to the r and g probabilities, the molecule C reacts to give E and S or E and P. If C does not react, the probability motion is checked. When accepted, a random direction is picked and all neighbouring sites are analysed. The displacement will take place only if not impeded by another molecule.

- if the selected molecule is P, a destination site is chosen randomly within the 6 neighbouring positions; if this site is empty or occupied with S or P, the molecule moves to the new position; if it is occupied by E, C or O, the molecule rests in the old position.

A time step t is defined as the repetition of this Monte Carlo sequence for $N_{tot}(t)$ times, where $N_{tot}(t)$ is the total number of mobile molecules in the lattice at the time t. Each simulation run has 1000 time steps. The computed values of the reactants concentrations and

15

of the rate coefficients are averaged over 200 to 500 independent runs. For all our calculations the time is expressed in simulation time units and the concentrations of the reactants are expressed as ratios between the number of particles and the number of all lattice sites, being thus coincident with their densities. In our model, the crowding is produced only by the big molecules (O) and can be evaluated considering the excluded volume, ϕ. It is calculated as the product between the particle concentration, its size (expressed in number of occupied sites) and the lattice dimension.

In order to analyse the effects of obstacle concentration and size, we have considered in our simulations a constant initial concentration of reactants (enzyme, [E]=0.0002 and substrate, [S]=0.01), and four distinct obstacles concentrations for each of their size to reach the same excluded volume, $\varphi = 0.1, 0.2, 03, 0.4$.

3.2 Fitting procedure

After the previously described simulations are run we obtain the values of the rate constants k_1, k_{-1} and k_2 over time, this procedure being explained elsewhere [40, 52, 57]. In order to test if the proposed Eq. 4 is valid to describe the temporal dependence of k_1 and further to determine the values of the equation parameters, we plot k_1 versus time and perform the fitting. To be as accurate as possible, the fitting is done after the curves are adjusted by excluding the points corresponding to the initial steps in which the reaction is very fast because the substrate concentration has not achieved yet a stationary profile (a necessary condition required to obtain the well-known diffusion-limited rate constant given by Eq. 7). We use the Levenberg-Marquardt non-linear fitting procedure with our Eq. 4 under the Origin 8.5 software package (OriginPro, OriginLab Corp.). The fitting is performed until the chi-squared (χ^2) test values cannot be minimized anymore.

4. Results and discussions

4.1 Diffusion-limited reactions

First, we study the case of diffusion-limited reactions, $f = 1$. The simulation data represent the values of the rate coefficients k_1, k_{-1} and k_2 over time and the concentrations of every type of molecule implicated in the reaction for each time step. The rate constants k_{-1} and k_2 do not correspond to diffusion controlled reactions, they are constant and the linear fitting of the corresponding data yielded the imposed probabilities, $k_{-1} = 0.02$ and $k_2 = 0.04$ (Fig.1a). Of the most interest for our study are the curves of k_1 versus time. The general shape of the curves can be seen in Fig.1a, which shows the case of [S] = 0.02, [E] = 0.0001 and ϕ = 0.3 for obstacles of size 5x5x5 R. The curve presents a sharp decrease at the beginning followed by a gradual decrease in time, underlining the fractal type of kinetics. As mentioned above, the initial steps correspond to a rapid reaction taking place before the achievement of the stationary profile of the substrate molecules, favoured by a homogeneous distribution of the reactants due to the random arrangement of the molecules at the beginning of the simulation. Due to crowding, diffusion is impeded and thus the collisions between reactants are diminished, reflected by the decrease of k_1 versus time. Fig. 1b shows the dependence of $\log(k_1)$ on time for the case without obstacles. It has a constant behaviour, as expected, with a lower value that that obtained in presence of obstacles.

The time dependence of reactant and product concentration is shown in Fig. 2, for the case of [S] = 0.02, [E] = 0.0001 and ϕ = 0.4 for obstacles of size 3x3x3. It can be noticed that enzyme, E, and complex, C, concentrations show a sharp variation at initial times and then follow a monotonic one. This is determined by the reactions occurring at the beginning of the simulation when all molecules are randomly distributed. Then, the reactions follow without achieving a stationary state, until they stop due to consumption of substrate molecules. Additionally, it is worth mentioning here the log-log plot of k_1 versus time that allows us to see the reaction process from another point of view (Fig. 3). There are four regions within this

17

plot. The first decreasing part, very steep, corresponds to the initial steps of the rapid reaction previously discussed. The second one is a plateau in which k_1 is almost constant in time as it happens in classical kinetics. Therefore, we can interpret that the Michaelis-Menten reaction shows a classical behaviour during this time interval. The third and the fourth regions of the plot are characteristic to the fractal kinetics with the last one corresponding to a linear decrease of $\log(k_1)$ versus $\log(t)$ as described by the limiting behaviour expressed in Eq. 6.

It should be noted here that the proposed Eq. 4 not only describes the two limit linear regions of the plot but also the transition curve between them. This is to say, that this equation contains and links two limit expressions: $k_1 = k_0 \, (\text{for } t << \tau)$ and $k = k_0^{\cdot} \cdot t^{-h} \, (\text{for } t >> \tau)$. The log-log plot allows the determination of the crossover time value, τ, which corresponds to the passage from one limiting expression to another. It may also be estimated as the time value related to the intersection of the two linear fittings of the linear regions (see Fig. 3).

In order to assign an interpretation to this temporal dependence of k_1 the proposed Eq. 4 has been used as the fitting function. Within a plot, considering all data points, the fitting has not brought a good representation. Therefore, the curves have been adjusted in such a way to remove the data corresponding to the initial steps (see the fitted curve in Fig. 4). To be able to identify that particular point we have considered the graph that gives the complex concentration of each case versus time. The curve presents a maximum, reached shortly after the simulation starts, which might be seen as the end of these initial steps (Fig. 4).

As a result, we have chosen the time corresponding to this maximum value of the complex concentration as the initial time for the fitting procedure. After the fitting, we have retrieved the values of k_0, h and τ parameters of Eq. 4 for all the investigated cases, as presented in Table 1, which also shows χ^2 for the goodness of the fit. To study the influence of crowding and obstacles size on the temporal dependence of k_1, we have analysed the way in which these factors influence the values of k_0, h and τ parameters (see Table 1).

18

The physical meaning of the parameters of Eq. 4 helps in understanding the non-classical kinetic behaviour of the system. The k_0 parameter is the rate constant associated to the diffusion limited reaction at short periods of time when the reaction occurs in a confined volume. The h parameter has the same meaning as that given by Kopelman [6], a fractal parameter that reflects two aspects: the fractality of the media and the spectral dimension of the random walk of the particles in that medium. The τ parameter might be regarded not as the time after the reaction "feels" the crowding effects [40] but as the crossover time between two particular regimes that system goes through, the classical one in which k_1 is constant and the fractal one that follows Kopelman's equation, Eq. 1.

Figure 5 shows the variation of rate coefficient, k_1, for different obstacles sizes for the same excluded volume, $\phi = 0.4$. The k_0 values retrieved from the curves (Table 1) increase along with the obstacle size. This variation might be interpreted in terms of the finite volume where the reactants are confined. In crowded media the reactants are initially confined in a small volume and the rate constant increases as the confined volume decreases according to Eq. 14.

Figures 6 and 7 comparatively present the k_1 time dependence for the same excluded volume in the presence of different obstacles size. The obtained k_0 values (Table 1) present distinct variations. In the case in which the smallest obstacles are present, the k_0 value decreases for higher excluded volumes. On the contrary, for cases with bigger obstacles, k_0 value rises along with the excluded volume. This result is expected as the confined volume diminishes, being consistent with Eq. 14 predictions.

In order to explain the reaction rate dependence on obstacle size for the same excluded volume and the dependence distinct behaviour on the excluded volume for cases with small and big obstacles, respectively, we focus on the confined volume meaning. Previous simulations of enzyme diffusion in crowded media [19] present that the crossover length,

$r* \equiv \sqrt{\tau * D_E^*}$, has a similar behaviour. The crossover length values computed in our study are shown in Table 2. It can be seen that for all cases with obstacles bigger than 1x1x1 size, the crossover length becomes smaller as the exclude volume rises, yielding a decreased confined volume and an increased value of the initial rate constant, k_0. The opposite behaviour for the case of 1x1x1 obstacles size is probably due to a greater proportion of obstacle cluster [9]. Moreover, for the same excluded volume, the crossover length becomes higher for bigger obstacles explaining the rise of k_0 value. The behaviour of both rate coefficient and crossover length illustrate that the enzyme-obstacle relative size is a very important factor for *in vivo* enzymatic reactions. Moreover, a small substrate-enzyme relative size against the obstacles favours a higher initial rate.

Regarding the crossover time, τ, it links with the crossover length because it relates to the time that reactants (E and S) are present in confined volumes and need to further diffuse to continuous confined volumes. Table 1 presents the obtained values of this crossover time, but with higher errors than the other parameters, due to a less precise way to determine it. This crossover time decreases, for the same excluded volume, if the obstacle size grows. Thus, this parameter becomes important when quantifying the initial period of time in which the enzymatic reaction is enhanced and acts as in dilute solution.

The interpretation of τ parameter comes out from the log-log plots of k_1 versus time. The equation that we have proposed provides a good description of the fractal regime and, additionally, it contains and links two limit expressions corresponding to short and large periods of time: $k_1 = k_0$ (for $t << \tau$) and $k_1 = k_o^{'} t^{-h}$ (for $t >> \tau$). This ensures the meaning of a crossover time for τ. The τ values drop sharply for higher exclude volume reflecting in this way that the transition from classical to fractal regime, described by Kopelman's equation, occurs at shorter periods of time.

Concerning the *h* parameter, we note that its values are small (Table 1), probably due to the fact that anomalous diffusion is imperceptible in the studied cases and also that the reaction occurs in a 3D media. The *h* values increase with the obstacle concentration, being thus in agreement with the fact that it represents the media fractality. This fact is also seen in Figs. 5 to 7 in which the fractal regions slopes change with obstacle concentration. These regions are described by Kopelman's Eq. 1 that in log-log representation gives *h* as the slope of the lines. Moreover, the values obtained for this parameter do not depend on obstacle size but only on the exclude volume. This behaviour does not correlate with the variation of anomalous diffusion exponent, α, obtained in our previous simulation of enzymes diffusion [20].

It is important to mention that the estimation of the parameters of Eq. 4 (k_0, τ and *h*) is susceptible to be influenced by the limits brought by the usage of a 3D squared lattice. The reduced anisotropy of the considered grid may lead to minor changes of the parameters values as revealed by Grima and Schnell [55] when comparing the results obtained from on- and off-lattice 2D simulations.

Depending on the temporal scale, the macromolecular crowding may have positive or negative effects on the reaction kinetics. For short periods of time, macromolecular crowding stimulates reaction because the reactants are confined and they need to explore a small volume in order to meet each other and react. For large periods of time (and at long distances), the decrease of the reactants diffusion coefficients diminishes the rate of collisions between them and thus it decreases the value of the rate coefficient.

4.2 Mixed activation-diffusion reactions

In this section, we study the case of mixed activation-diffusion reactions, *f* = 0,75; 0,5; 0,25. We chose the case of maximum value of the excluded volume below the percolation threshold, ϕ = 0.4. The fitting values of the parameters of Eq. 4 (k_0, τ and *h*) are shown in

Table 3. The results obtained gives that the rate constant, k_0, diminishes as the probability of reaction, f, as expected, because the reaction passes from a diffusion-limited to a mixed activation-diffusion control as happens in classic kinetics for bimolecular reactions [68]. The fractality, h, also diminishes, due to the fact that it is associated to the obstructed diffusion process in crowded media. Finally, the crossover time, τ, also decreases until have a negligible value, which is normal because in the mixed activation-diffusion control the time that the substrate and enzyme need to react is not important in order to react. This behaviour is observed in the high errors found for the fitted crossover time to Eq. 4. Alternatively, the crossover time, τ, can be obtained if we only fit the values of k_1 for long periods of time ($t \gg \tau$), so the third region in Fig. 3, with Kopelman's equation (6). We obtain the values of h and $k_o^{'}$ parameters and we may estimate the crossover time using the relationship given in Eq. 6, $\tau = \left(k_0^{'}/k_0\right)^{1/h}$. The values of τ are shown in Table 4 with the fitted values to Kopelman's equation, for cases of the highest excluded volume, $\phi = 0.4$, considered here, and for obstacle size of 3x3x3. Now, the standard errors for τ diminish, but they are large enough, indicating that the time dependence of rate constant for bimolecular reactions in crowded media decreases as the mixed activation-diffusion control increases, until to not have sense. This could means that in the cases of activation control, the crowding only affects to the value of bimolecular rate constants, probably due to different surroundings seen by the substrate and enzyme molecules when react, and also for possible conformation changes of the enzyme [16].

22

Acknowledgments

References

[1] S.B. Zimmerman, A.P. Minton, Macromolecular crowding: biochemical, biophysical and physiological consequences, Annu. Rev. Biophys. Biomol. Struct. 22 (1993) 27.

[2] A.P. Minton, The influence of macromolecular crowding and macromolecular confinement of biochemical reactions in physiological media, J. Biol. Chem. 276 (2001) 10577.

[3] D. Hall, A.P. Minton, Macromolecular crowding: qualitative and semiquantitative successes, quantitative challenges, Biochim. Biophys. Acta. 1649 (2003) 127.

[4] M.J. Saxton, Lateral diffusion in a mixture of mobile and immobile particles. A Monte Carlo study, Biophys. J 58 (1990) 1303.

23

[5] M.J. Saxton, Lateral diffusion in archipelago. Dependence on tracer size, Biophys. J 64 (1993) 1053.

[6] M.J. Saxton, Anomalous diffusion due to obstacles: A Monte Carlo study, Biophys. J 66 (1994) 394.

[7] B.P. Olveczky, A.S. Verkman, Monte Carlo analysis of obstructed diffusion in three dimensions: Application to molecular diffusion in organelles, Biophys. J. 74 (1998) 2722.

[8] A.S. Verkman, Solute and macromolecule diffusion in cellular aqueous compartments, Trends Biochem. Sci. 27 (2002) 27.

[9] M. Weiss, M. Elsner, F. Kartberg, T. Nilsson, Anomalous subdiffusion is a measure for cytoplasmic crowding in living cells, Biophys. J 87 (2004) 3518.

[10] M.J. Saxton, A biological interpretation of transient anomalous subdiffusion. I. Qualitative model, Biophys. J. 92 (2007) 1178.

[11] A. Isvoran, E. Vilaseca, J.L. Garces, L. Unipan, and F. Mas, Simulation of diffusion in two-dimensional crowded media, Proceedings of the 6th Conference of Balkan Physics Union, American Institute of Physics Journal 889 (2007) 469.

[12] A. Isvoran, E. Vilaseca, L. Unipan, J.L. Garces, and F. Mas, Monte Carlo simulation of single particle-diffusion in two-dimensional and three-dimensional crowded media, Romanian J. Biophys. 17 (2007) 21.

[13] G. Guigas, M. Weiss, Sampling the cell with anomalous diffusion. The discovery of slowness, Biophys. J. 94 (2008) 90.

[14] M.J. Saxton, A biological interpretation of transient anomalous subdiffusion. II. Reaction kinetics, Biophys. J. 94 (2008) 760.

[15] Dix, J. A.; Verkman, A. S. Crowding effects on diffusion in solutions, Annu. Rev. Biophys. 37 (2008) 247.

[16] H.X. Zhou, G. Rivas and A. Minton, Macromolecular Crowding and Confinement: Biochemical, Biophisical and Potential Physiological Consequences, Annu. Rev. Biophys. 37 (2008) 375.

[17] A. Isvoran, E. Vilaseca, L. Unipan, J.L. Garcés and F. Mas, Computational study of diffusion in cellular two-dimensional crowded media modelled as mixtures of mobile and immobile obstacles, Rev. Roumaine Chim. 53 (2008) 415.

[18] I. Pastor, E. Vilaseca, S. Madurga, J.L. Garcés, M. Cascante and F. Mas, Diffusion of α–Chymotrypsin in Solution-Crwoded Media. A Fluorescence Recovery after Photobleaching Study, J. Phys. Chem. 114 (2010) 4028; erratum, ibid, 114 (2010) 12182.

[19] E. Vilaseca, A. Isvoran, S. Madurga, I. Pastor, J.L. Garcés and F. Mas, New insights into diffusion in 3D crowded media by Monte Carlo simulations: effect of size, mobility and spatial distribution of obstacles, Phys. Chem. Chem. Phys. 13 (2011) 7396.

[20] E. Vilaseca, I. Pastor, A. Isvoran. S. Madurga, J.L. Garcés and F. Mas, Diffusion in macromolecular crowded media: Monte Carlo simulation of obstructed diffusion *vs.* FRAP experiments, Theor. Chem. Acc. 128 (2011) 795.

[21] T.C. Laurent, Enzyme Reactions in Polymer Media, Eur. J. Biochem. 21 (1971) 498.

[22] Wenner, J. R.; Bloomfield, V. A. Crowding Effects on EcoRV Kinetics and Binding, Biophys. J. 77 (1999).

[23] Asaad, N.; Engberts, J. B. F. N. Cytosol-Mimetic Chemistry: Kinetics of the Trypsin-Catalyzed Hydrolysis of p-Nitrophenyl Acetate upon Addition of Polyethylene Glycol and N-tert-Butyl Acetoacetamide, J. Am. Chem. Soc. 125 (2003) 6874.

[24] Derham, B. K.; Harding, J. J. The effect of the presence of globular proteins and elongated polymers on enzyme activity, Biochim. Biophys. Acta 1746 (2006) 1000.

[25]   Olsen, S. N. Applications of isothermal titration calorimetry to measureenzyme kinetics and activity in complex solutions, Thermochim. Acta 448 (2006) 12.

[26]   Homchaudhuri, L.; Sarma, N.; Swaminathan, R. Effect of crowding by Dextrans and Ficolls on the rate of alkaline phosphatase-catalyzed hydrolysis: a size-dependent investigation, Biopolymers 83 (2006) 477.

[27]   Olsen, S. N.; Raml¢v, H.; Westh, P. Effects of osmolytes on hexokinase kinetics combined with macromolecular crowding Test of the osmolyte compatibility hypothesis towards crowded systems, Comp. Biochem. Physiol. A 148 (2007) 339.

[28]   Moran-Zorzano, M. T.; Viale, A.; Muñoz, F.; Alonso-Casajas, N.; Eydaltm, G. et al. Escherichia coli AspP activity is enhanced by macromolecular crowding and by both glucose-1,6-bisphosphate and nucleotide-sugars, FEBS Lett. 581 (2007) 1035.

[29]   Jiang, M.; Gou, Z. H. Effects of Macromolecular Crowding on the Intrinsic Catalytic Efficiency and Structure of Enterobactin-Specific Isochorismate Synthase, J. Am. Chem. Soc. 129 (2007) 730.

[30]   Norris, M.G.S.; Malys N. What is the true enzyme kinetics in the biological system? An investigation of macromolecular crowding effect upon enzyme kinetics of glucose-6-phosphate dehydrogenase, Biochem. Biophys. Res. Commun. 405 (2011) 388.

[31]   Verma, P. K.; Rakshit, S.; Mitra, R. K.; Pal, S. K. Role of hydration on the functionality of a proteolític enzyme α-chymotrypsin under crowded environment, Biochimie 93 (2011) 1424.

[32]   Hou, S.; Ziebacz, N.; Kalwarczyk, T.; Kaminski, T. S.; Wieczoreka, S. A.; Holyst, R. Influence of nano-viscosity and depletion interactions on cleavage of DNA by enzzymes

in glicerol and poly(ethylene glycol) solutions: qualitative analysis, Soft Matter 7 (2011) 3092.

[33]   I. Pastor, E. Vilaseca, S. Madurga, J.L. Garcés, M. Cascante and F. Mas, Effect of Crowding by Dextrans on the Hydrolysis of N-Succinyl-L-phenil-Ala-p-nitroanilide Catalyzed by α–Chymotrypsin, J. Phys. Chem. B 115 (2011) 1115.

[34]   Akabayov, S. R.; Akabayov, B.; Richardson, C. C.; Wagner, G. Molecular crowding enhanced ATPase actuvity of the RNA helicase eIF4A correlates with compaction of its quaternari structure and association with eIF4G, JACS 135 (2013) 10040.

[35]   Akabayov, B.; Akabayov, S. R.; Lee, S. J.; Wagner, G.; Richardson, C. C. Impact of macromolecular crowding on DNA replication, Nat. Commun. 4 (2013) 1615.

[36]   Liu, J.; Peng, J.; Shen, S.; Jin, Q.; Li, C.; Yang, Q. Enzyme entrapped in polímer-modified nanopores: the effects of macromolecular crowding and surface hydrophobicity, Chem. Eur. J. 19 (2013) 2711.

[37]   Pitulice, L.; Pastor, I.; Vilaseca, E.; Madurga, S.; Isvoran, A.; Cascante, M.; Mas, F. Influence of macromolecular crowding on the oxidation of ABTS by hydrogen peroxide catalyzed by HRP, J Biocatal Biotransformation 2 (2013) 1.

[38]   I. Pastor, L. Pitulice, C. Balcells, E. Vilaseca, S. Madurga, A. Isvoran, M. Cascante, F. Mas, Effect of crowding by Dextrans in enzymatic reactions, Biophys. Chem. 185 (2014) 8.

[39]   C. Balcells, I. Pastor, E. Vilaseca, S. Madurga, M. Cascante, F. Mas, Macromolecular crowding effect upon *in* vitro enzyme kinetics: mixed activation-diffusion control of the

reduction of Pyruvate by NADH catalysed by Lactate Dehydrogenase induced by Dextrans, submitted.

[40]   S. Schnell, T.E. Turner, Reaction kinetics in intracellular environments with macromolecular crowding, Progr. Biophys. Mol. Biol. 85 (2004) 235.

[41]   R. Kopelman, Rate processes on fractals: theory, simulations and experiments, J. Stat. Phys. 42 (1986) 185.

[42]   R. Kopelman, Fractal reaction kinetics, Science 241 (1988) 1620.

[43]   M.A. Savageau, Michaelis-Menten mechanism reconsidered: implications on fractal kinetics, J. Theor. Biol. 176 (1995) 115.

[44]   Z. Bajzer, M. Huzak, K.L. Neff and F.G. Prendergast, Reaction kinetics in intracellular environments: the two proposed models yield qualitatively different predictions, Croatica Chem. Acta 79 (2006) 437.

[45]   Z. Bajzer, M. Huzak, K.L. Neff and F.G. Prendergast, Mathematical analysis of models for reaction kinetics in intracellular environments, Math. Biosci. 215 (2008) 35.

[46]   K.L. Neff, Ch.P. Offord, A.J. Claride, E.E. Strehler, F.G. Prendergast and Z. Bajzer, Validation of fractal-like kinetic models by time-resolved binding kinetics of dansylamide and carbonic anhydrase in crowded media, Biophys. J. 100 (2011) 2495.

[47]   T.E. Turner, S. Schnell, and K. Burrage, Stochastic approaches for modeling in vivo reactions, Comput. Biol. Chem. 28 (2004) 165.

[48]   T. Tian, K. Burrage, Stochastic models for regulatory networks of the genetic toggle switch, PNAS 103 (2006) 8372.

[49]   J. Wu, B. Vidakovic, E.O. Voit, Constructing stochastic models from deterministic process equations by propensity adjustment, BMC, Systems Biology 5 (2011) 187.

[50]   M.R. Riley, M.M. Buettner, F.J. Muzzio, and C.S. Reyes, Monte Carlo simulation of diffusion and reaction in two-dimensional cell structure, Biophys. J. 68 (1995) 1716.

[51] A. Lin, R. Kopelman, Nonclassical kinetics in three dimensions: simulations of elementary A+B and A+A reactions, Phys. Rev. E. 53 (1996) 1502.

[52]   H. Berry, Monte Carlo simulations of enzyme reactions in two dimensions: fractal kinetics and spatial segregation, Biophys. J. 83 (2002) 1891.

[53]   K. Kosmidis, V. Karalis, P. Argyrakis, and P. Macheras, Michaelis Menten kinetics under spatially constrained conditions: application to the mibefradil pharmacokinetics, Biophys. J. 87 (2004) 1498.

[54]   C.J. Roussel, M.R. Roussel, Reaction-diffusion models of development with state dependent chemical diffusion coefficients, Progr. Biophys. Mol. Biol. 86 (2004) 113-160

[55]   R. Grima, S. Schnell, A systematic investigation of the rate laws valid in intracellular environments, Biophys. Chem. 124 (2006) 1.

[56]   R. Grima, Intrinsic biochemical noise in crowded intracelular conditions, J. Chem. Phys. 132 (2010) 185102.

[57] A. Isvoran, E. Vilaseca, F. Ortega., M. Cascante, and F. Mas, About implementing a Monte Carlo simulation algorithm for enzymatic reactions in crowded media, J. Serb. Chem. Soc. 71 (2006) 75.

[58] A. Isvoran, E. Vilaseca, J.L. Garcés, L. Unipan and F. Mas, Nonclassical kinetics for enzymatic reactions in two-dimensional media, Romanian Biophys. J. 18 (2008) 283.

[59] M. Agrawal, S. B. Santra, R. Anand and R. Swaminathan, Effect of macromolecular crowding on the rate of diffusion-limited enzymatic reaction, PRAMANA. Journal of Physics 71(2008) 359.

[60] M.T. Klann, A. Lapin and M. Reuss, Agent-based simulation of reactions in the crowded and structured intracellular environment: Influence of mobility and location of the reactants, BMC Systems Biology 5 (2011) 71.

[61] C. Echevería, K. Tucci and R. Kapral, Diffusion and reaction in crowded environments, J. Phys. Condens. Matter 19 (2007) 1.

[62] S. Park and N. Agmon, Theory and Simulation of Diffusion-Controlled Michaelis-Menten Kinetics for a Static Enzyme in Solution, J. Phys. Chem. B 112 (2008) 5977.

[63] J.S. Kim and A. Yethraj, Effect of Macromolecular Crowding on Reaction rates: A computational and Theoretical Study, Biophys. J. 96 (2009) 1333.

[64] J.X. Chen and R. Kapral, Mesoscopic dynamics of diffusion-influenced enzyme kinetics, J. Chem. Phys. 134 (2011).

[65] G.N. Wei and Q.L. Zou, Enzyme Kinetics in Crowded Cellular Environment, Asian J. Chem. 24 (2012) 3917.

[66] T. Vopel, G.I. Makhatadze, Enzyme Activity in the Crowded Milieu, PLoS ONE, 7 (2012) e39418.

[67] L. Pitulice, Fractal aspects of the structure and dynamics of biomolecules, PhD Thesis, West Timisoara University, Timisoara (Romania), 2009.

[68] P. Atkins, J. de Paula, Physical Chemistry, 8th Ed. Oxford University Press, New York, 2006.

[69] R. Alsallaq, H.X. Zhou, Electrostatic rate enhancement and transient complex of protein-protein association, Proteins 71 (2008) 320.

[70] G. Schreiber, G. Haran, H.X. Zhou, Fundamental Aspects of Protein-Protein Association Kinetics, Chem. Rev. 109 (2009) 839.

[71] A. Bar-Even, E. Noor, Y. Savir, W. Liebermeister, D. Davidi, D. S. Tawfik, R. Milo, The moderately efficient enzyme: evolutionary and physicochemical trends shaping enzyme parameters, Biochem. 50 (2011) 4402.

Table 1. The values of k_0, h and τ dimensionless parameters for all the cases under study with

$f = 1$.

Obstacle size	ϕ	k_0	τ	h	χ^2
1x1x1	0.1	1.49±0.01	64±37	0.0072±0.0002	2.558
	0.2	1.42±0.01	43±26	0.0087±0.0002	2.243
	0.3	1.33±0.01	24±18	0.0111±0.0002	1.964
	0.4	1.21±0.02	12±10	0.0174±0.0002	1.555
3x3x3	0.1	1.62±0.01	36±31	0.0071±0.0002	3.068
	0.2	1.70±0.01	57±29	0.0088±0.0002	3.300
	0.3	1.81±0.02	17±17	0.0110±0.0002	3.727
	0.4	1.88±0.01	34±15	0.0144±0.0002	3.869
5x5x5 R	0.1	1.65±0.01	24±29	0.0069±0.0002	3.162
	0.2	1.74±0.01	56±29	0.0087±0.0002	3.577
	0.3	1.87±0.01	21±18	0.0109±0.0002	4.009
	0.4	1.97±0.01	39±16	0.0142±0.0002	4.455
7x7x7 R	0.1	1.66±0.01	27±30	0.0069±0.0002	3.208
	0.2	1.79±0.01	31±25	0.0086±0.0002	3.766
	0.3	1.93±0.01	29±19	0.0108±0.0002	4.288
	0.4	2.08±0.01	36±16	0.0141±0.0002	4.947

Table 2. The values of dimensionless k_0 and τ in comparison with crossover length, r^*, for all the cases under study with $f = 1$

Obstacle size	ϕ	k_0	r^*
1x1x1	0.1	1.49±0.01	5.09
	0.2	1.42±0.01	5.53
	0.3	1.33±0.01	6.04
	0.4	1.21±0.02	6.31
3x3x3	0.1	1.62±0.01	9.19
	0.2	1.70±0.01	8.62
	0.3	1.81±0.02	8.57
	0.4	1.88±0.01	8.34
5x5x5 R	0.1	1.65±0.01	12.27
	0.2	1.74±0.01	10.96
	0.3	1.87±0.01	9.72
	0.4	1.97±0.01	8.91
7x7x7 R	0.1	1.66±0.01	14.95
	0.2	1.79±0.01	13.54
	0.3	1.93±0.01	12.31
	0.4	2.08±0.01	10.81

33

Table 3. The values of k_0, h and τ dimensionless parameters for cases with exclude volume ϕ = 0.4 and different values of f

Obstacle size	f	k_0	τ	h	χ^2
1x1x1	1	1.21±0.02	12±10	0.0174±0.0002	1.554
	0.75	1.0±0.2	2±31	0.0113±0.0004	4.640
	0.5	0.7±0.2	2±52	0.0075±0.0004	2.972
	0.25	-	-	-	-
3x3x3	1	1.88±0.01	34±15	0.0144±0.0002	3.869
	0.75	1.5±0.3	1±39	0.0085±0.0004	10.084
	0.5	1.1±0.2	2±63	0.0053±0.0004	5.666
	0.25	0.61±1.4	0.1±127	0.0018±0.0004	2.353
5x5x5 R	1	1.97±0.01	39±16	0.0142±0.0002	4.455
	0.75	1.6±0.2	3±43	0.0081±0.0004	11.312
	0.5	1.2±0.2	2±75	0.0045±0.0004	6.031
	0.25	0.6±0.5	0.4±184	0.0017±0.004	2.435
7x7x7 R	1	2.08±0.01	36±16	0.0141±0.0002	4.947
	0.75	1.7±0.2	3±43	0.0079±0.0004	12.668
	0.5	1.2±0.2	3±76	0.0047±0.0004	6.787
	0.25	-	-	-	-

34

Table 4. The values of $k_0^{'}$, h and τ dimensionless parameters obtained from Kopelman equation (6) for cases with exclude volume $\phi = 0.4$ and obstacle size 3x3x3 for different values of f

Obstacle size	f	$k_0^{'}$	h	$\tau = \left(k_0^{'}/k_0\right)^{1/h}$	χ^2
3x3x3	1	1.977±0.003	0.0144±0.0002	34±74	3.719
	0.75	1.545±0.005	0.0079±0.0004	0.7±22	9.542
	0.5	1.105±0.004	0.0042±0.0004	0.2±16	5.310
	0.25	0.601±0.002	0.0006±0.0005	$(10^{-9}\text{-}10^{-6})$	2.191

Figure captions

Fig. 1

(a) Time dependence of k_1 and constant values of k_{-1} and k_2 for the case with 3x3x3 obstacles and an excluded volume of 0.4; (b) Comparison of time dependence of $\log(k_1)$ versus $\log(t)$ between the case of obstacles given in (a) and the case without obstacles.

Fig. 2

Time evolution of the substrate, product, enzyme and complex concentrations for the case with 3x3x3 obstacles and an excluded volume of 0.4

Fig. 3

The $\log(k_1)$ versus $\log(t)$ plot for the case with 3x3x3 obstacles and an excluded volume of 0.4

Fig. 4

Indication of the fitting starting points for the time dependence curves of k_1 and complex concentration for the case with 3x3x3 obstacles and an excluded volume of 0.4. Fitted curve of k_1 is plotted in continuos line.

Fig. 5

The log-log plots of k_1 versus time for the four considered obstacle sizes and the excluded volume of 0.4

Fig. 6

The log-log plots of k_1 versus time for all considered values of excluded volume when the obstacle size is 1x1x1.

Fig. 7

The log-log plots of k1 versus time for all considered values of excluded volume when the obstacle size is 7x7x7 R.
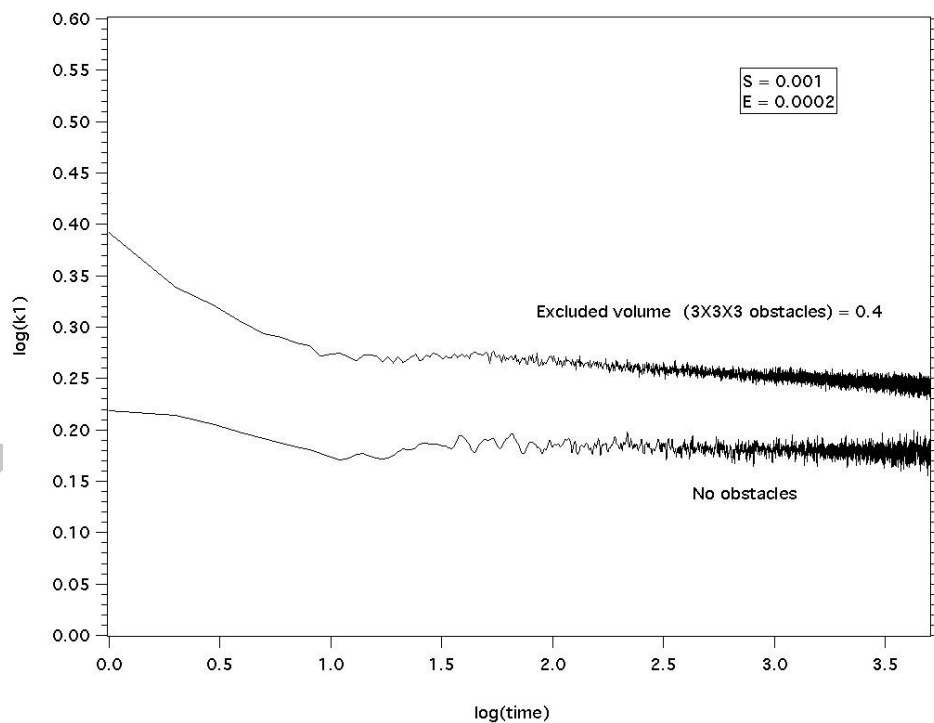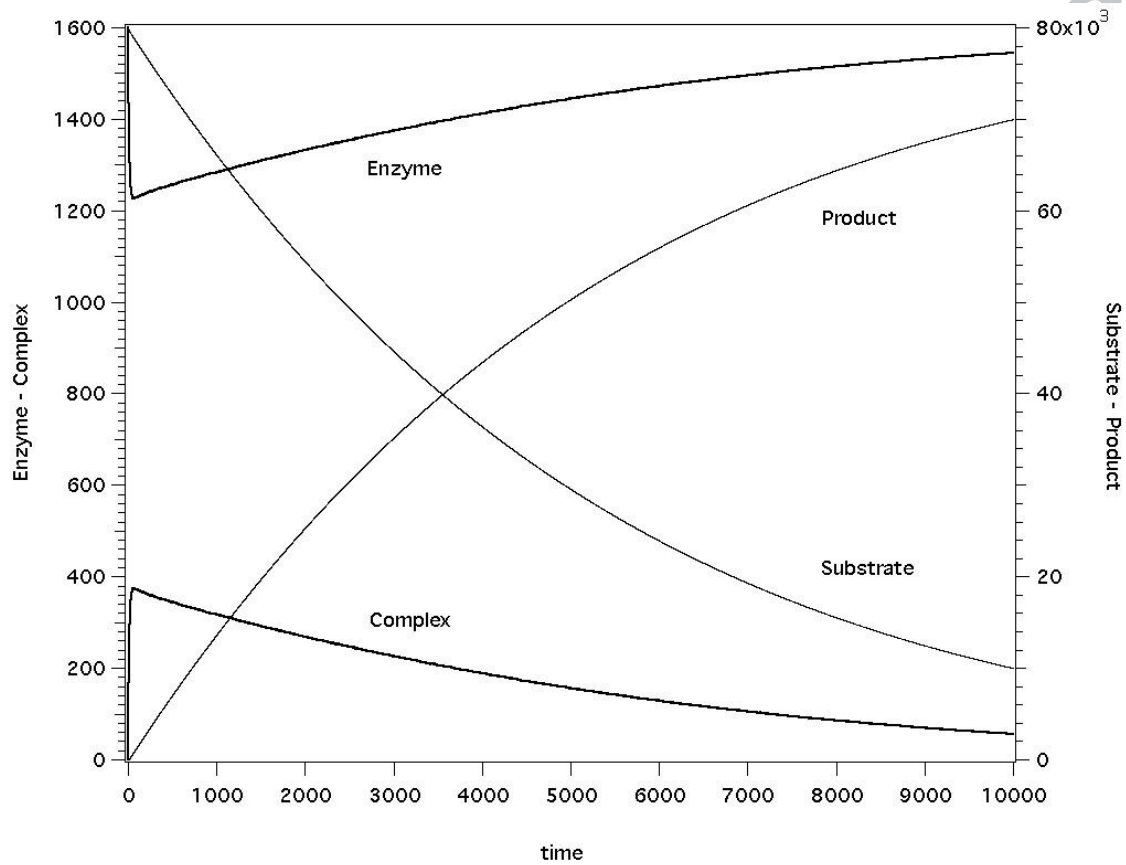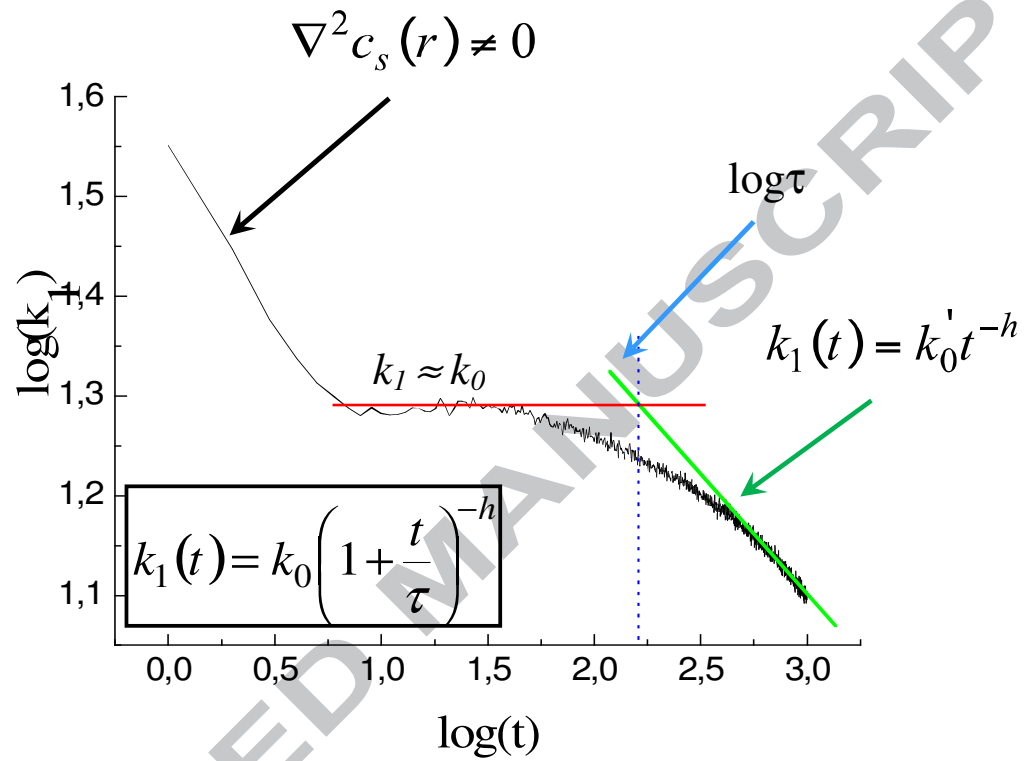
Fig. 1a
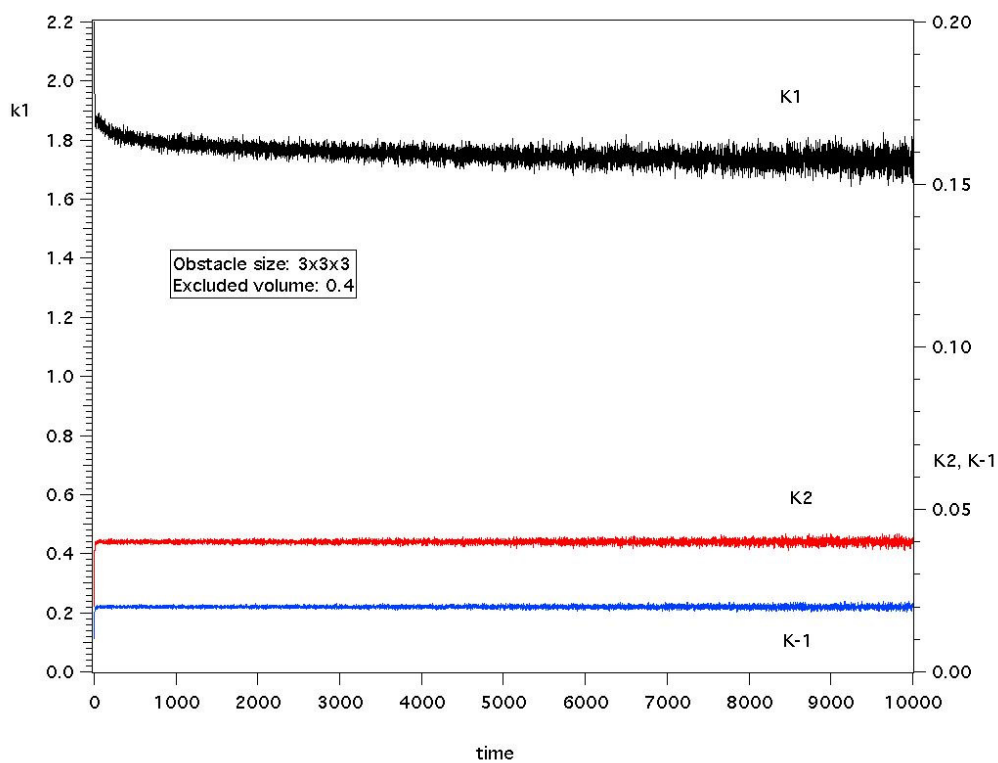
Fig. 1b

Fig. 2

Fig. 3

$$\nabla^2 c_s(r) \neq 0$$

$$k_1 \approx k_0$$

$$\log\tau$$

$$k_1(t) = k_0^{'} t^{-h}$$

$$k_1(t) = k_0\left(1 + \frac{t}{\tau}\right)^{-h}$$
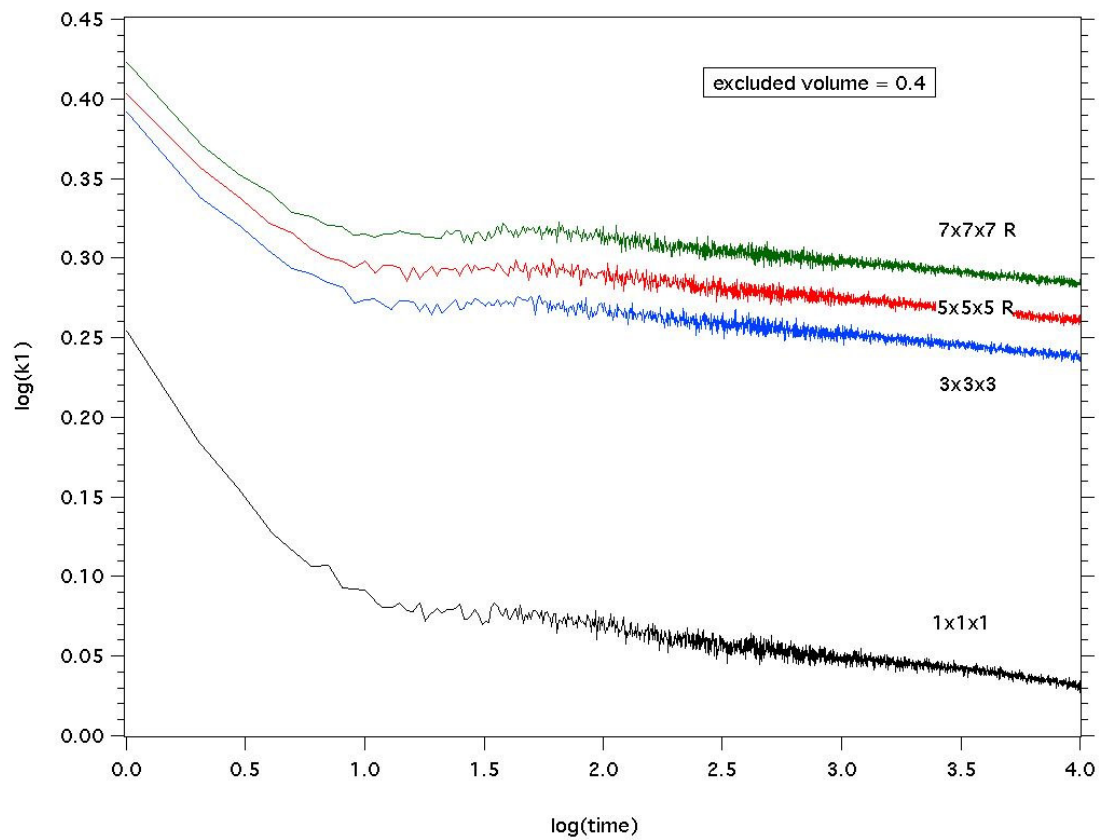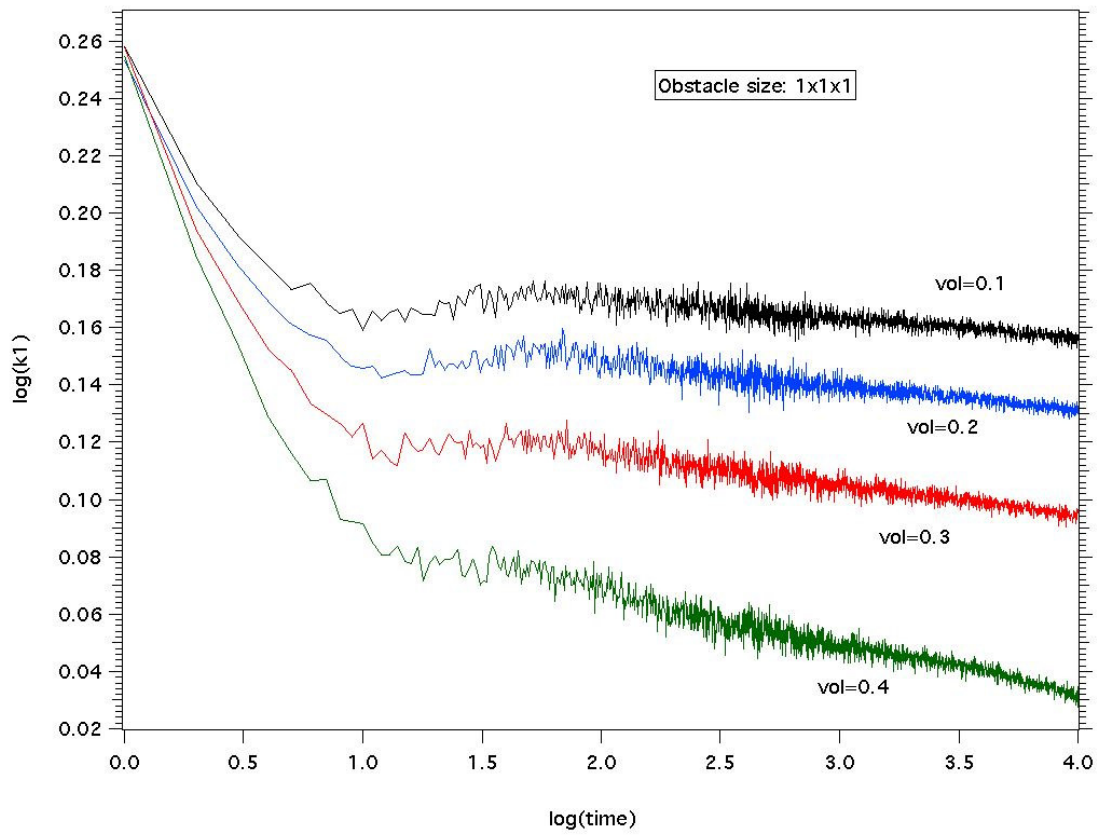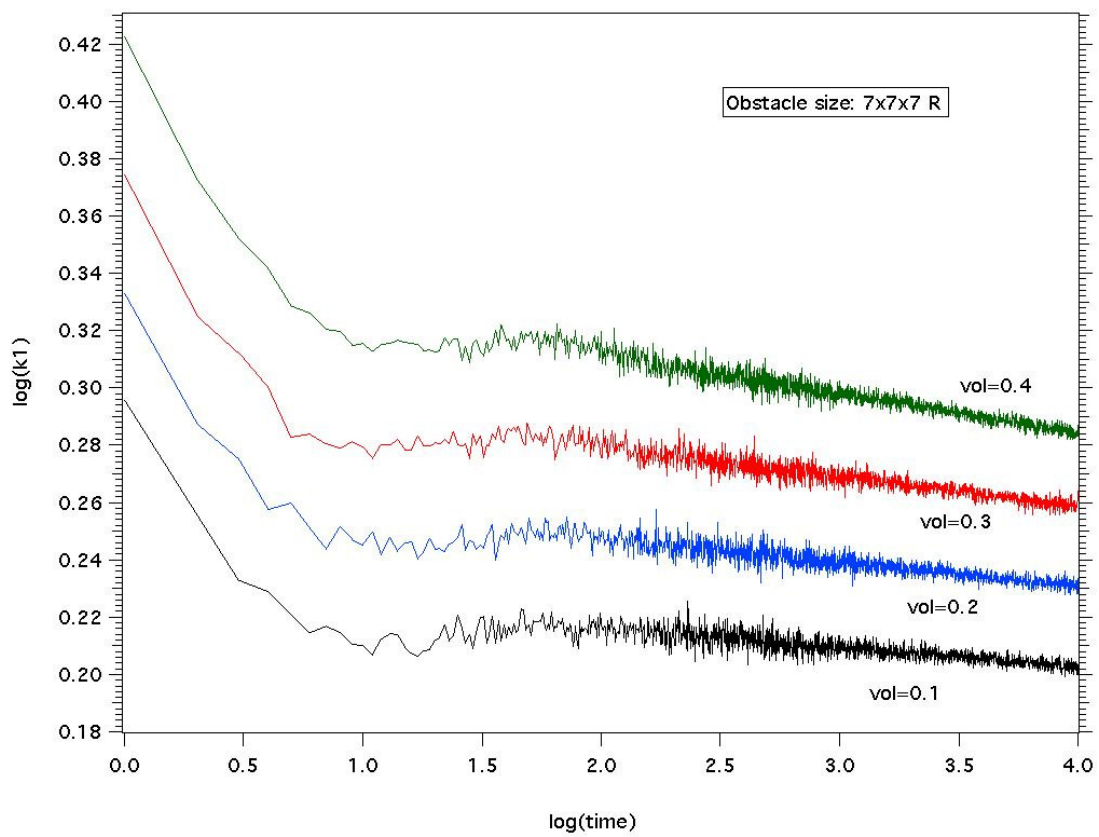
log(k₁) axis: $\log(k_1)$

log(t) axis: $\log(t)$

Fig. 4
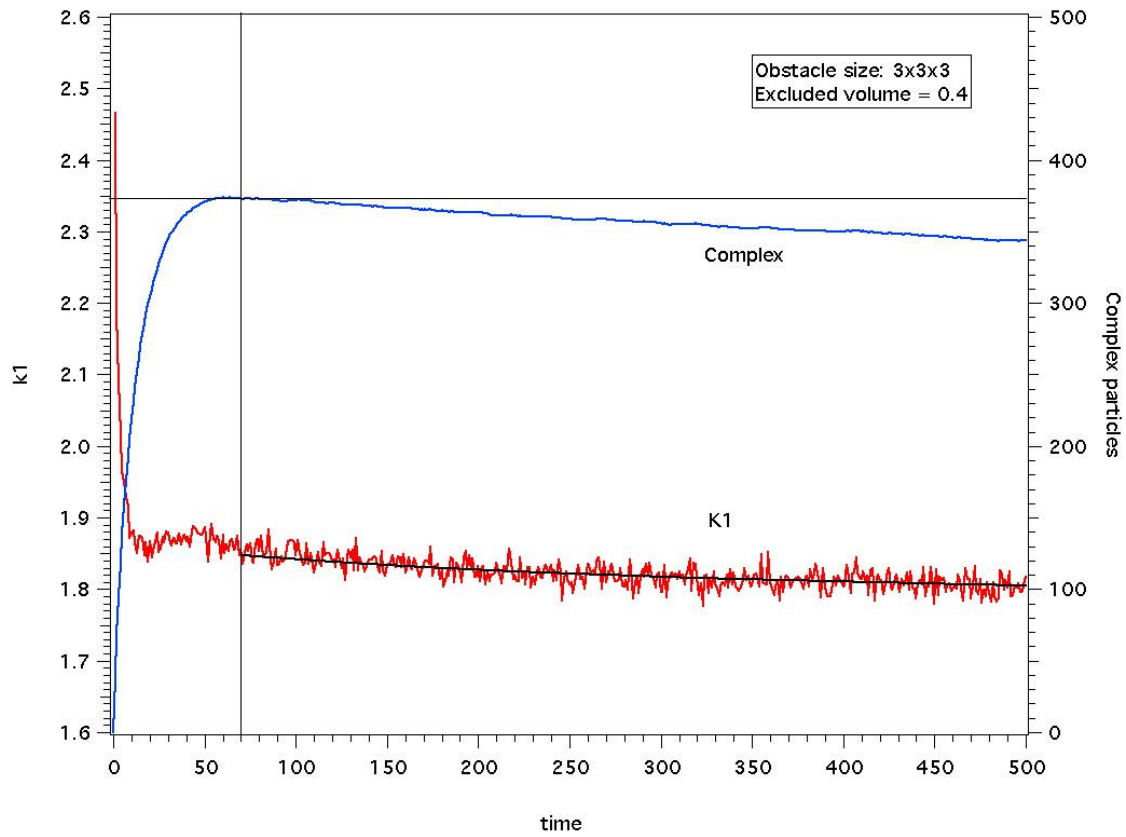
Fig. 5

Fig. 6

Fig. 7

Highlights of the paper "Monte Carlo simulations of enzymatic reactions in crowded media. Effect of the enzyme-obstacle relative size"

- The study reveals a fractal kinetics of enzymatic reactions in 3D crowded media
- A modified equation is proposed to describe the fractal kinetics
- The parameters of proposed equation are interpreted
- The dependence of kinetics fractality on the excluded volume is explained
- Kinetics fractality dependence on reactants-obstacles relative size in also provided